International Journal of Thermophysics, Vol. 13, No. 2, 1992

Monte Carlo Studies of Multiwavelength Pyrometry Using Linearized Equations

G. R. Gathers[1]

Received June 10, 1991

Multiwavelength pyrometry has been advertised as giving significant improvement in precision by overdetermining the solution with extra wavelengths and using least squares methods. Hiernaut et al. [1] have described a six-wavelength pyrometer for measurements in the range 2000 to 5000 K. They use the Wien approximation and model the logarithm of the emissivity as a linear function of wavelength in order to produce linear equations. The present work examines the measurement errors associated with their technique.

KEY WORDS: high temperatures; multiwavelength pyrometry; pyrometry, temperature measurements.

1. INTRODUCTION

Hiernaut et al. [1] have described a six-wavelength pyrometer for measurements in the range 2000 to 5000 K. Hiernaut et al. [2] used this instrument to measure the melting point and emissivity of refractory metals. They assume the Wien approximation and take the logarithm of the emissivity as a linear function of wavelength. They obtain six equations relating the measured intensities at the six wavelengths to the spectral model. The pairwise combination of these equations to eliminate the constant term in the emissivity model gives 15 independent equations. Chi-square fits using the 15 equations allows a linear least-squares determination of the temperature and the wavelength coefficient for the logarithm of the emissivity. Back substitution then determines the constant term. The present work uses the Monte Carlo method to examine the precision of the technique, its dependence on the spectral span of the wavelengths chosen, the choice of

[1] Lawrence Livermore National Laboratory, University of California, Livermore, California 94550.

0195-928X/92/0300-0361$06.50/0

weight function used in the χ^2 fit, and the degree of improvement achieved by using multiple wavelengths to overdetermine the solution. Since Hiernaut et al. [2] observed the emissivity to be either an increasing or a decreasing function of wavelength, depending on temperature, both situations are examined. In addition, the effect of using logarithmic amplifiers is considered.

2. MATHEMATICAL DEVELOPMENT

We assume from the outset that the Wien approximation is an adequate approximation to the Planck spectrum for the temperature range of interest. For linear amplifiers, we take the output voltage V_i for channel i proportional to the intensity $J_R(\lambda_i, T)$ through a transfer function A_i:

$$V_i = A_i J_R(\lambda_i, T) = A_i \varepsilon(\lambda_i)\, c_1 e^{-c_2/\lambda_i T}/\lambda_i^5 \tag{1}$$

where c_1 and c_2 are the standard radiation constants and we assume

$$\ln \varepsilon(\lambda_i) = a_0 + a_1 \lambda_i \tag{2}$$

For convenience, set $A_i = 1$. For brevity, let us define

$$R_i = J_R(\lambda_i, T) \tag{3}$$

and

$$\beta_i = \ln(\lambda_i^5 R_i / c_1) \tag{4}$$

We then have

$$\beta_i = a_0 + a_1 \lambda_i - c_2/\lambda_i T \tag{5}$$

Define the difference

$$\varphi_{ij} = (\beta_i - \beta_j)/(\lambda_i - \lambda_j) = a_1 + c_2/T\lambda_i\lambda_j \tag{6}$$

Let $a_2 = c_2/T$ so that we can write

$$\varphi_{ij} = a_1 + a_2/\lambda_i\lambda_j \tag{7}$$

For n channels, we have $n(n-1)/2$ independent equations of the form given by Eq. (7):

$$\varphi_{ij} = a_1 + a_2/\lambda_i\lambda_j, \qquad i = 1,..., n-1, \quad j = i+1,..., n \tag{8}$$

We define chi-squared as

$$\chi^2 = \sum_{i=1}^{n-1} \sum_{j=i+1}^{n} \frac{1}{\sigma_{ij}^2} (\varphi_{ij}^* - a_1 - a_2/\lambda_i\lambda_j)^2 \tag{9}$$

Where the asterisk denotes values obtained from measurements, and σ_{ij}^2 is the variance of φ_{ij}^*. We minimize χ^2 with respect to a_1 and a_2:

$$\frac{\partial \chi^2}{\partial a_1} = -2 \sum_{i=1}^{n-1} \sum_{j=i+1}^{n} \frac{1}{\sigma_{ij}^2} (\varphi_{ij}^* - a_1 - a_2/\lambda_i\lambda_j) = 0 \tag{10}$$

$$\frac{\partial \chi^2}{\partial a_2} = -2 \sum_{i=1}^{n-1} \sum_{j=i+1}^{n} \frac{1}{\sigma_{ij}^2} (\varphi_{ij}^* - a_1 - a_2/\lambda_i\lambda_j)/\lambda_i\lambda_j = 0 \tag{11}$$

We have

$$\vec{G} = \mathbf{M} \cdot \vec{a} \tag{12}$$

Where

$$G_1 = \sum_{i=1}^{n-1} \sum_{j=i+1}^{n} \frac{1}{\sigma_{ij}^2} \varphi_{ij}^*, \qquad G_2 = \sum_{i=1}^{n-1} \sum_{j=i+1}^{n} \frac{1}{\sigma_{ij}^2} \frac{\varphi_{ij}^*}{\lambda_i\lambda_j}$$

$$M_{11} = \sum_{i=1}^{n-1} \sum_{j=i+1}^{n} \frac{1}{\sigma_{ij}^2}, \qquad M_{12} = M_{21} = \sum_{i=1}^{n-1} \sum_{j=i+1}^{n} \frac{1}{\sigma_{ij}^2} \frac{1}{\lambda_i\lambda_j} \tag{13}$$

$$M_{22} = \sum_{i=1}^{n-1} \sum_{j=i+1}^{n} \frac{1}{\sigma_{ij}^2} \frac{1}{(\lambda_i\lambda_j)^2}, \qquad \vec{a} = (a_1, a_2)$$

Solution may be obtained for a_1 and a_2 by Gauss elimination, then

$$a_0 = \beta_1^* - a_1\lambda_1 + a_2/\lambda_1 \tag{14}$$

and finally,

$$T = c_2/a_2 \tag{15}$$

2.1. Linear Amplifiers

$$V_i = A_i R_i \tag{16}$$

so that

$$\beta_i = \ln(\lambda_i^5 V_i / c_1 A_i) \tag{17}$$

Now to first order

$$\sigma_{\beta_i}^2 = \left(\frac{\partial \beta_i}{\partial V_i}\right)^2 \sigma_i^2 \tag{18}$$

where σ_i^2 is the variance of the voltage V_i.

$$\frac{\partial \beta_i}{\partial V_i} = 1/V_i \tag{19}$$

so that

$$\sigma_{\beta_i}^2 = (\sigma_i/V_i)^2 \tag{20}$$

Also, to first order, we have

$$\sigma_{ij}^2 = \left(\frac{\partial \varphi_{ij}}{\partial \beta_i}\right)^2 \sigma_{\beta_i}^2 + \left(\frac{\partial \varphi_{ij}}{\partial \beta_j}\right)^2 \sigma_{\beta_j}^2 \tag{21}$$

Where we assume the voltage measurements in the channels are independent of each other. The β_i are thus uncorrelated, and there is no covariance. From Eq. (6) we have

$$\frac{\partial \varphi_{ij}}{\partial \beta_i} = 1/(\lambda_i - \lambda_j) \tag{22}$$

and

$$\frac{\partial \varphi_{ij}}{\partial \beta_j} = -1/(\lambda_i - \lambda_j) \tag{23}$$

Substituting, we obtain

$$\sigma_{ij}^2 = (\sigma_{\beta_i}^2 + \sigma_{\beta_j}^2)/(\lambda_i - \lambda_j)^2 \tag{24}$$

Substituting Eq. (20) we have

$$\sigma_{ij}^2 = [(\sigma_i/V_i)^2 + (\sigma_j/V_j)^2]/(\lambda_i - \lambda_j)^2 \tag{25}$$

Now consider the case of constant relative errors:

$$\sigma_i = \omega V_i \tag{26}$$

where ω is a constant. We have

$$\sigma_{ij}^2 = 2\omega^2/(\lambda_i - \lambda_j)^2 \tag{27}$$

and the factor $2\omega^2$ will factor out of χ^2, so that we can write

$$\chi^2 = \sum_{i=1}^{n-1} \sum_{j=i+1}^{n} (\lambda_i - \lambda_j)^2 (\varphi_{ij}^* - a_1 - a_2/\lambda_i\lambda_j)^2 \tag{28}$$

Now consider the case where the errors are equal to a constant fraction of the maximum signal seen in a channel, as when determined by trace width on an oscilloscope or discriminator spacing with a digital recorder.

$$\sigma_i = \omega V_i(\max) \tag{29}$$

We have

$$(\sigma_i/V_i)^2 = \omega^2 (V_i(\max)/V_i)^2 \tag{30}$$

$$\sigma_{ij}^2 = \frac{\omega^2}{(\lambda_i - \lambda_j)^2} [(V_i(\max)/V_i)^2 + (V_j(\max)/V_j)^2] \tag{31}$$

and again, the factor of ω^2 will factor out of χ^2.

2.2. Logarithmic Amplifiers

We assume

$$V_i = A_i \ln R_i \tag{32}$$

We have

$$\ln R_i = \ln(c_1/\lambda_i^5) + a_0 + a_1\lambda_i - a_2/\lambda_i = \beta_i \tag{33}$$

We again have Eq. (9) with φ_{ij} defines as before. Solution for a_0, a_1, and T follow the same path.

Now

$$\beta_i = \ln(\lambda_i^5/c_1) + \ln R_i = \ln(\lambda_i^5/c_1) + V_i/A_i \tag{34}$$

We see that the relationship between V_i and β_i has changed.

$$\frac{\partial \beta_i}{\partial V_i} = 1/A_i \tag{35}$$

so that

$$\sigma_{\beta_i}^2 = \left(\frac{\partial \beta_i}{\partial V_i}\right)^2 \sigma_i^2 = (\sigma_i/A_i)^2 \tag{36}$$

and we have

$$\sigma_{ij}^2 = \frac{1}{(\lambda_i - \lambda_j)^2} [(\sigma_i/A_i)^2 + (\sigma_j/A_j)^2] \tag{37}$$

Now consider the case of constant relative errors given by Eq. (26). We have

$$\sigma_i/A_i = \omega V_i/A_i \tag{38}$$

or

$$\sigma_{ij}^2 = \frac{\omega^2}{(\lambda_i - \lambda_j)^2} [(V_i/A_i)^2 + (V_j/A_j)^2] \tag{39}$$

For convenience, we take the case $A_i = A = \text{constant}$, so that

$$\sigma_{ij}^2 = (\omega/A)^2 (V_i^2 + V_j^2)/(\lambda_i - \lambda_j)^2 \tag{40}$$

$(\omega/A)^2$ will factor out of χ^2 and have no effect on the relative weights.

Now consider the case where the errors are proportional to the maximum signal seen in a channel (and the same fraction for each channel)

$$\sigma_i = \omega V_i(\max) \tag{41}$$

$$\sigma_i/A_i = \omega V_i(\max)/A_i \tag{42}$$

and we have

$$\sigma_{ij}^2 = \frac{\omega^2}{(\lambda_i - \lambda_j)^2} [(V_i(\max)/A_i)^2 + (V_j(\max)/A_j)^2] \tag{43}$$

As before, consider $A_i = A = \text{constant}$, so that $(\omega/A)^2$ will factor out of χ^2. We have

$$\sigma_{ij}^2 = \frac{1}{(\lambda_i - \lambda_j)^2} [V_i^2(\max) + V_j^2(\max)] \tag{44}$$

3. CODE METHODS

A generator code was written to create exact artificial data for a linear ramp of temperature versus time and for a given pyrometer configuration (wavelengths, amplifier type). A random number generator is then used to alter the exact data for the specified type of error and create artificial data in batches for a large number of runs. A random seed is used at the

beginning of each run. A data reduction code then reduces the batches of data, leaving a dropfile of the results, to be evaluated by a third code which does the statistical analysis.

Experiments were made using 100 runs and 500 runs. Since we have a ramp of results versus time (or true temperature), curve-fitting methods can be used to smooth the results for 100 runs. The smoothed results were in good agreement with the trials using 500 runs. It is thus possible to reduce the amount of computer time used for a problem by about a factor of five by using 100 runs and curve-fitting methods. Overall, best results are generally obtained by least-squares fitting a quadratic to the results. The reduction in computer time needed makes it possible to explore more variables.

Two methods were used to calculate the emissivity at each time point. The mean values of a_0 and a_1 were determined at each point and used to calculate the emissivity for each wavelength at that time. The emissivity $\varepsilon[\bar{a}_0(t_i), \bar{a}_1(t_i), \lambda_k]$ is thus calculated. As an alternative, the emissivity for every run, wavelength, and time point was calculated and averaged over runs at a given time point to give $\bar{\varepsilon}(t_i, \lambda_k)$. It was found that the technique of averaging a_0 and a_1 first gives better results, and it was thus chosen. As a result, however, the true standard deviation of the emissivity cannot be calculated. Instead, the percentage deviation of ε from the smoothed result is used. A quadratic fit to the amplitude of the percentage deviation of ε from the smoothed value is also made to give further smoothing. These results are also plotted as a function of true temperature for each wavelength.

Two types of random error are considered. The first considers 2% uniformly distributed random relative errors (every artificial exact data voltage is multiplied by a random number uniformly distributed between 0.98 and 1.02). For this case a large range of temperature can be examined at one time. Since the Wien approximation is used, the range $1000 \leqslant T \leqslant 4000$ K was chosen. For the second case, which is more representative of experimental data, the errors introduced were in the range plus or minus 0.02 times the maximum signal seen in each channel. For this situation, the dynamic range considered must be restricted, since at low signal levels, the injected errors cannot be allowed to produce negative signals, for which there is no solution. The temperature range $3000 \leqslant T \leqslant 4000$ K was chosen. For convenience, we refer to this case as that of absolute errors.

Since the wavelength dependence of the emissivity has some influence on the results, two cases were considered: an emissivity that decreases with wavelength (characteristic of solid metals) from 0.5 at 500 nm to 0.2 at 1040 nm and one that increases with wavelength (characteristic of liquid metals) from 0.2 at 500 nm to 0.5 at 1040 nm.

Statistical improvement achieved by overdetermining the solution with extra wavelengths is examined by calculating the standard deviation of the temperature and the scatter in the emissivity at each wavelength for the cases of three, four, five, and six wavelengths. The importance of the weight function used in the χ^2 fit is also examined.

It has already been established that the use of logarithmic amplifiers is convenient for reducing the amount of recording equipment needed, but at the price of sacrificing precision. A few cases are thus examined using both linear and logarithmic amplifiers for comparison.

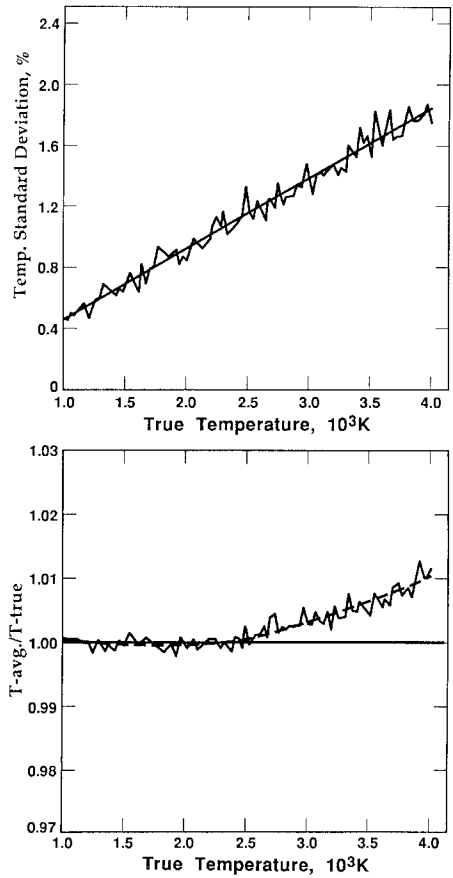

Fig. 1. Temperature results for six wavelengths, 500–1040 nm, linear amplifiers, $a_1 < 0$, and 2% uniformly distributed random relative errors, using unweighted fits.

4. RESULTS FOR RELATIVE ERRORS

4.1. Influence of Spectral Span

We consider six wavelengths, linear amplifiers, and unweighted fits in the χ^2 calculation.

4.1.1. Five Hundred to One Thousand Forty Nanometers

This corresponds to the configuration used by Hiernaut et al. [1]. Figure 1 shows the temperature results. The standard deviation for the

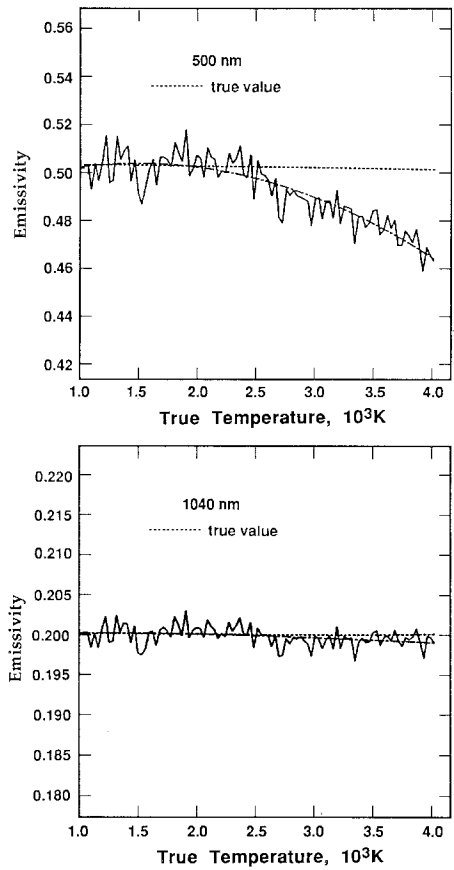

Fig. 2. Emissivity behavior for the extreme wavelengths, for six wavelengths, 500–1040 nm, linear amplifiers, $a_1 < 0$, and 2% uniformly distributed random relative errors, using unweighted fits.

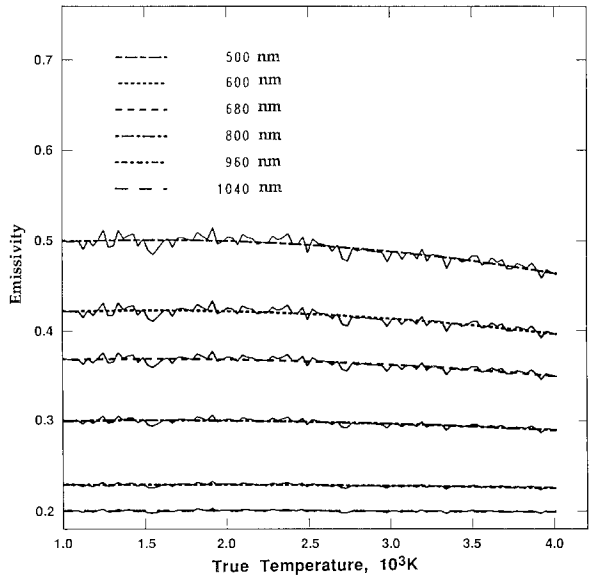

Fig. 3. Emissivity results for six wavelengths, 500–1040 nm, linear amplifiers, $a_1 < 0$, and 2% uniformly distributed random relative errors, using unweighted fits.

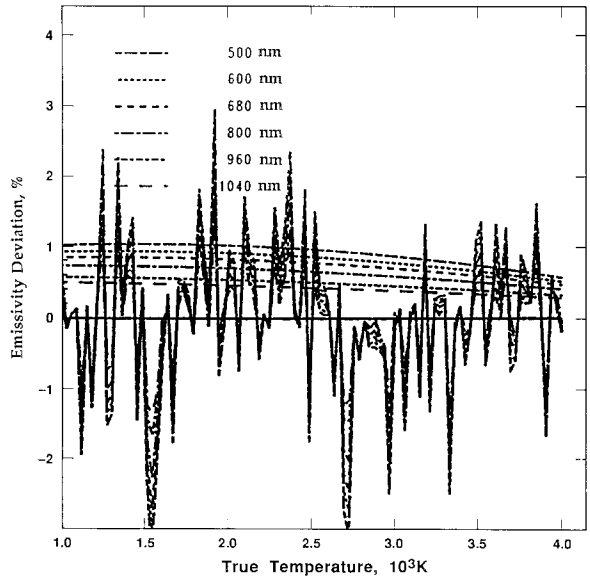

Fig. 4. Percentage deviation amplitude of emissivity from the smoothed values for six wavelengths, 500–1040 nm, linear amplifiers, $a_1 < 0$, and 2% uniformly distributed random relative errors, using unweighted fits.

temperature increases in an approximately linear fashion from 0.48% at 1000 K to 1.83% at 4000 K. The temperature shows an increasing bias upward to about 1% at 4000 K. Figure 2 shows the emissivity behavior for the two extreme wavelengths.

It can be seen that the emissivity rolls off about 7% at 4000 K for 500 nm. The effect is progressively less for the longer wavelengths. A simple analytical argument shows that the shift in both temperature and emissivity is due to the use of the Wien approximation. As confirmation, a problem was run substituting the Wien spectrum for the Planck spectrum in the generating code. The systematic shift completely disappeared. [In the

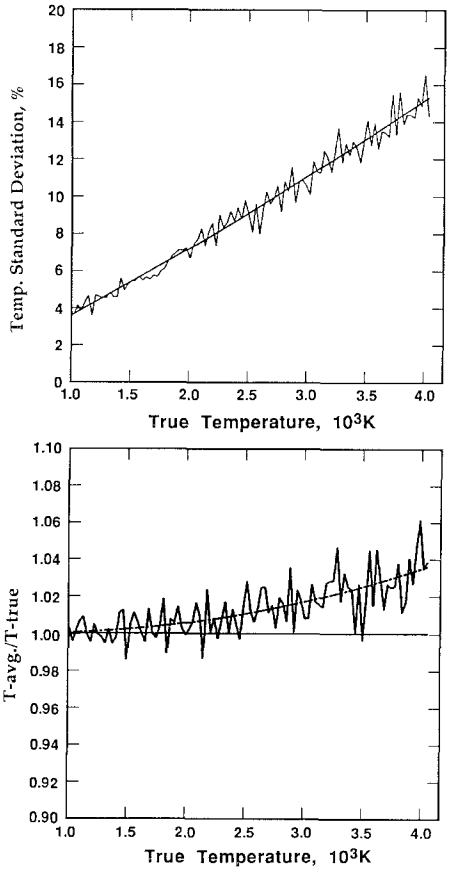

Fig. 5. Temperature results for six wavelengths, 680–900 nm, linear amplifiers, $a_1 < 0$, and 2% uniformly distributed random relative errors, using unweighted fits.

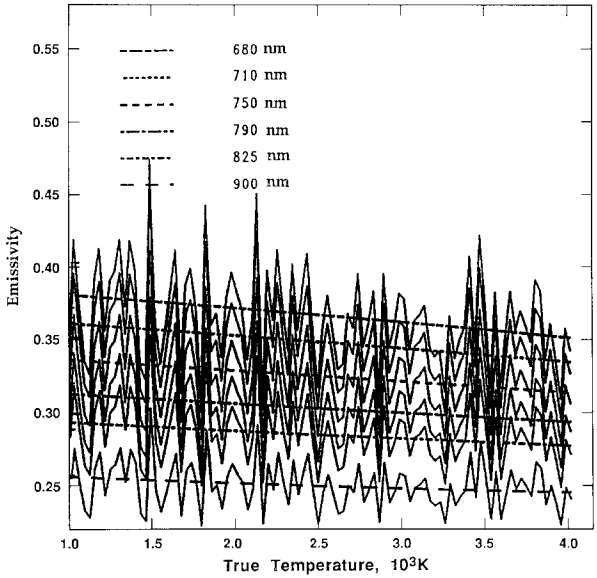

Fig. 6. Emissivity results for six wavelengths, 680–900 nm, linear amplifiers, $a_1 < 0$, and 2% uniformly distributed random relative errors, using unweighted fits.

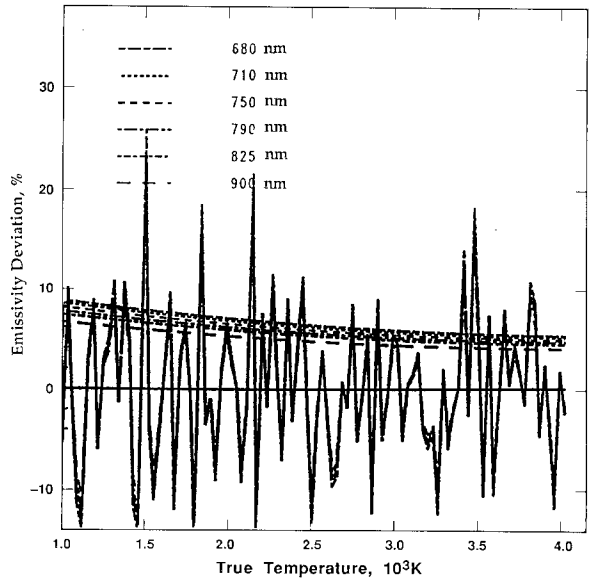

Fig. 7. Percentage deviation amplitude of emissivity from the smoothed values for six wavelengths, 680–900 nm, linear amplifiers, $a_1 < 0$, and 2% uniformly distributed random relative errors, using unweighted fits.

normal situation the generator code uses the Planck spectrum, since that is the true blackbody spectrum found in nature. Data reduction using the Wien approximation is an attempt to use the wrong spectrum to fit the data. If we (temporarily) use the Wien spectrum in the generator, the Wien approximation is no longer an approximation, and errors from this cause vanish.]

Figure 3 shows the emissivity behavior for all wavelengths. The greatest scatter occurs for the short wavelengths. At 1000 K the errors in the smoothed results are negligible. Figure 4 shows the percentage deviation of the emissivity from the smoothed result. The quadratic fits to the amplitude of the deviation are shown in the figure. It can be seen that

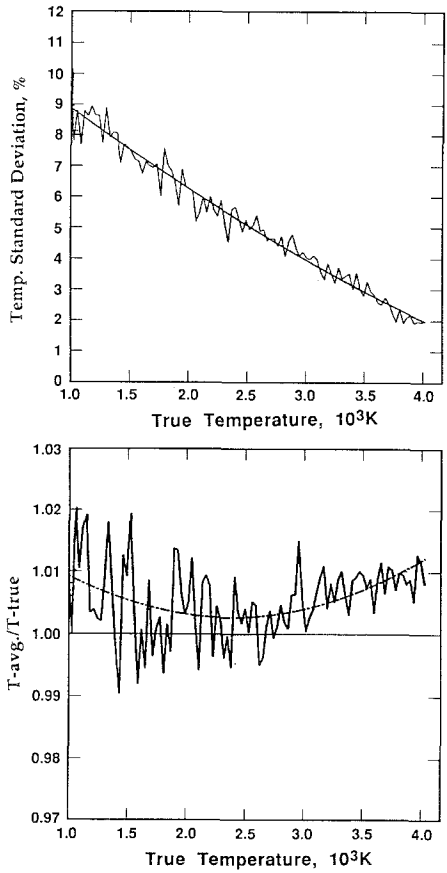

Fig. 8. Temperature results for six wavelengths, 500–1040 nm, logarithmic amplifiers, $a_1 < 0$, and 2% uniformly distributed random relative errors, using unweighted fits.

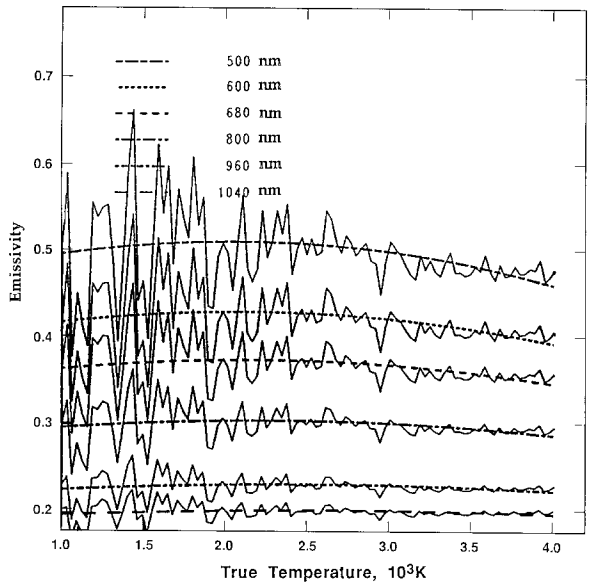

Fig. 9. Emissivity results for six wavelengths, 500–1040 nm, logarithmic amplifiers, $a_1 < 0$, and 2% uniformly distributed random relative errors, using unweighted fits.

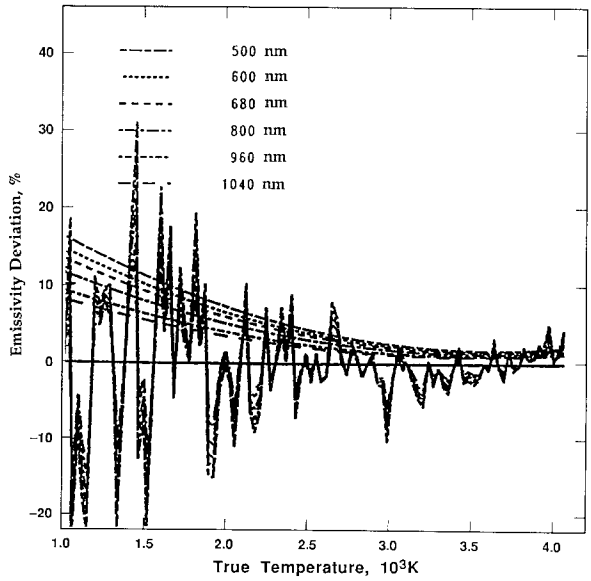

Fig. 10. Percentage deviation amplitude of emissivity from the smoothed values for six wavelengths, 500–1040 nm, logarithmic amplifiers, $a_1 < 0$, and 2% uniformly distributed random relative errors, using unweighted fits.

the worst case is about 1% for 500 nm at about 1000 K. The deviation is progressively less for the longer wavelengths. It may be noted that for a given temperature, the emissivities for the various wavelengths appear perfectly correlated. This is because the emissivity was calculated using $\varepsilon[\bar{a}_0(t_i), \bar{a}_1(t_i), \lambda_k]$ so that for each time point t_i, or temperature, the same values for a_0 and a_1 were used for each wavelength. In the generator code, every data point was altered separately so that there is actually no correlation between the data for different wavelengths.

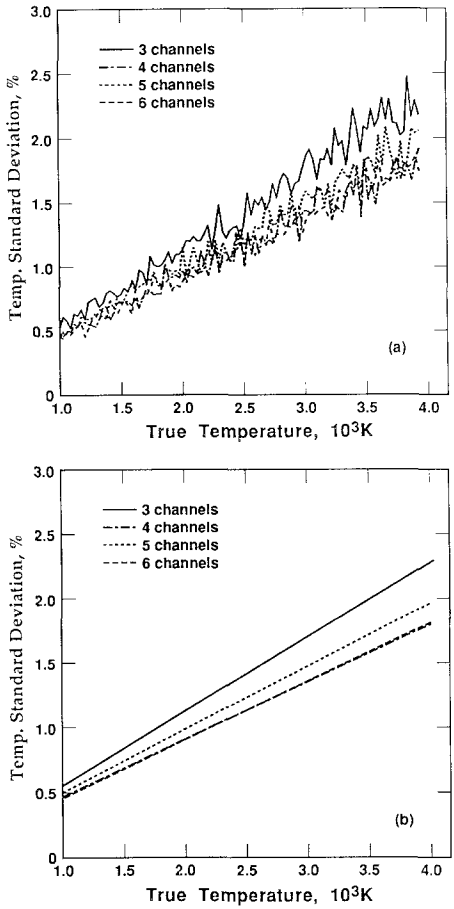

Fig. 11. Temperature standard deviation for three, four, five, and six wavelengths, 500–1040 nm, linear amplifiers, $a_1 < 0$, and 2% uniformly distributed random relative errors, using unweighted fits: (a) raw results; (b) results smoothed by fitting a quadratic.

4.1.2. Six Hundred Eighty to Nine Hundred Nanometers

Figure 5 shows the temperature results. The standard deviation has increased approximately eightfold at all temperatures. This is caused by a 60% decrease in spectral span. In addition, the systematic temperature error has increased more than threefold at 4000 K. Clearly this pyrometry technique is highly sensitive to spectral span. As a result, for studies of other variables, the spectral span was kept constant. Figure 6 shows the emissivity behavior, and Fig. 7 shows the degree of scatter in the emissivity

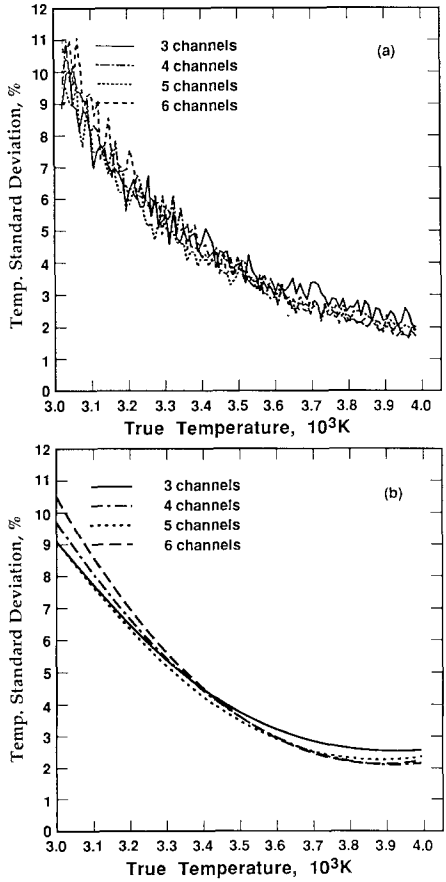

Fig. 12. Temperature standard deviation for three, four, five, and six wavelengths, 500–1040 nm, linear amplifiers, $a_1 < 0$, and errors proportional to 2% of the maximum signal for each channel, using unweighted fits: (a) raw results; (b) results smoothed by fitting a quadratic.

results. Both systematic error and scatter have increased markedly. The smoothed scatter ranges from 4% to about 8.5%.

4.2. Influence of Logarithmic Amplifiers

Again, we consider six wavelengths and unweighted fits, with a wavelength span from 500 to 1040 nm, and an emissivity decreasing with wavelength. Figure 8 shows the temperature results. The standard deviation varies from about 8.7% at 1000 K to about 2.0% at 4000 K. The upward bias of the temperature at 1000 K is probably not statistically significant.

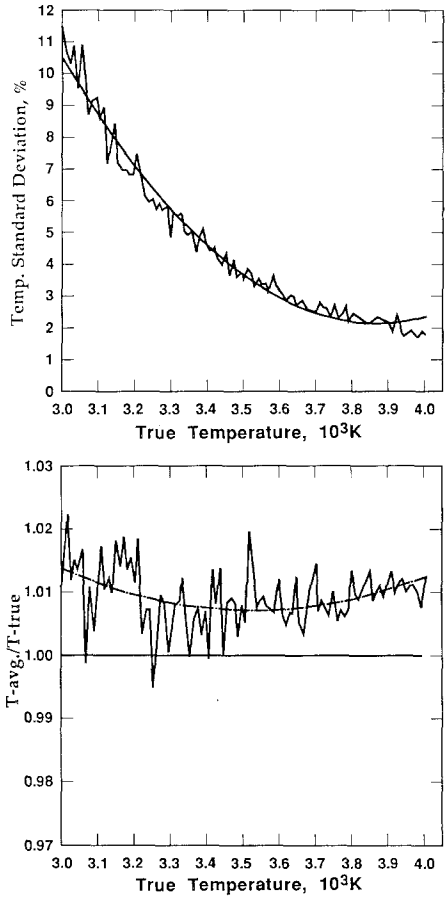

Fig. 13. Temperature results for six wavelengths, 500–1040 nm, linear amplifiers, $a_1 < 0$, and errors proportional to 2% of the maximum signal for each channel, using unweighted fits.

Figure 9 shows the emissivity behavior and Fig. 10 shows the degree of scatter. It is evident from comparison of Figs. 1, 3, and 4 with Figs. 8, 9, and 10 that the use of logarithmic amplifiers produces a significant penalty in precision, especially for the lower temperature signals. Again, the largest emissivity scatter is seen for the short wavelengths.

4.3. Influence of the Number of Wavelengths Used

For the problem considered in Figs. 1 through 4 with linear amplifiers, emissivity decreasing with wavelength, a spectral span from 500 to 1040 nm, and unweighted fits, smoothed and unsmoothed temperature standard deviations σ_T for three, four, five, and six wavelengths are shown as a function of temperature in Fig. 11. It can be seen that improvement in precision is not monotonic and little, if any, improvement is achieved beyond four wavelengths.

4.4. Influence of Weight Functions

The data used for the results shown in Figs. 1 through 4 were reprocessed using the correct weight functions. Only a slight improvement was

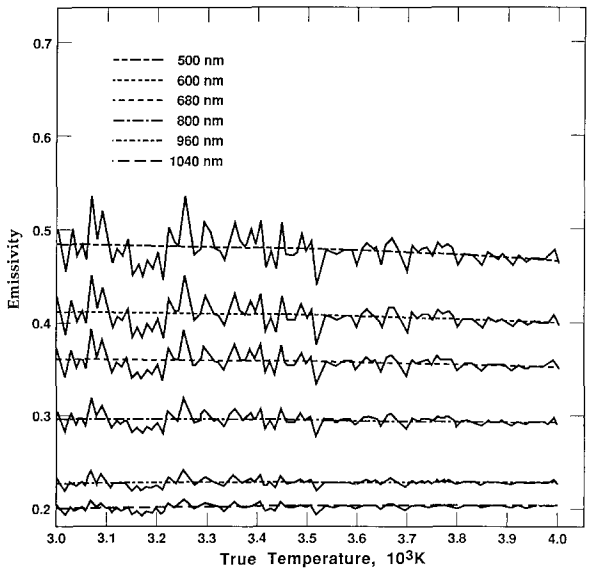

Fig. 14. Emissivity results for six wavelengths, 500–1040 nm, linear amplifiers, $a_1 < 0$, and errors proportional to 2 % of the maximum signal for each channel, using unweighted fits.

seen, and it is probably not statistically significant. The use of correct weight functions is thus not important for this scheme.

5. RESULTS FOR ABSOLUTE ERRORS

Again, we consider linear amplifiers, unweighted fits, and a spectral span from 500 to 1040 nm for three, four, five, and six wavelengths.

Figure 12 shows smoothed and unsmoothed σ_T versus temperature for three, four, five, and six wavelengths. Comparison of Figs. 11 and 12 shows that the character of the errors present is important. For absolute type errors, as expected, the largest percentage errors occur for the weakest signals, corresponding to the lower temperatures. In addition, there is no consistent statistical improvement achieved by adding additional wavelengths. Figure 13 shows the temperature behavior for six wavelengths. The combination of the results of the Wien approximation at the high temperatures and the increasing relative error at the low temperatures produces a bias of about $+0.8\%$ in the temperature. Figures 14 and 15 show the emissivity behavior. The increase in the scatter for short wavelengths and low temperatures is evident.

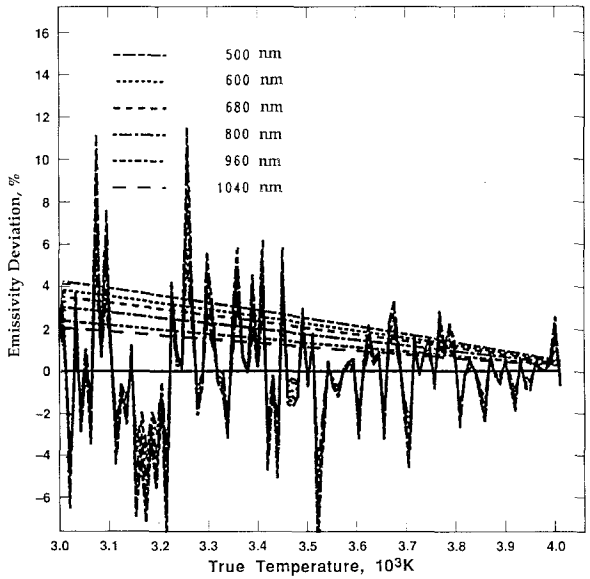

Fig. 15. Percentage deviation amplitude of emissivity from the smoothed values for six wavelengths, 500–1040 nm, linear amplifiers, $a_1 < 0$, and errors proportional to 2% of the maximum signal for each channel, using unweighted fits.

The influence of the weight functions for absolute errors was also found to be minor. In the χ^2 fits the equations for a_1 and a_2 are triangularized using Gauss elimination. The first variable obtained in the back substitution phase is a_2 (or the temperature), hence it is least sensitive to error. Detailed examination shows that use of the correct weight functions causes the left- and right-hand sides of the equation for a_2 to be multiplied by nearly equal numbers, so that the influence on results is minor.

6. COMPARISON WITH EXPERIMENT

Hiernaut et al. [2] show measurements of emissivity for tungsten as a function of temperature and wavelength. The largest scatter occurs for the shortest wavelengths and lowest temperatures. This is consistent with predictions for linear amplifiers and absolute type errors, as shown in Fig. 14.

7. CONCLUSIONS

This pyrometry method is quite sensitive to spectral span. For linear amplifiers and 2% uniformly distributed random relative errors, a 60% reduction in span causes the standard deviations to increase approximately eightfold. Statistical improvement achieved by overdetermining the solution with extra wavelengths is at best very minor, and does not increase monotonically with the number of wavelengths, for either type of error considered.

For typical experimental apparatus, the measured emissivities will have the greatest relative error for the lower temperatures (because of weaker signals there) and for the shortest wavelengths. This is in agreement with published results. The use of multiple recording devices with different sensitivities can be used to avoid large relative errors for the lower end of a temperature range considered.

The temperature errors produced by use of the Wien approximation are influenced by the spectral span. For 500–1040 nm, the calculated temperature at 4000 K is about 1% high. For 680–900 nm, it is about 3.5% high.

Unweighted fits may be used without significant degradation of results, and the results are insensitive to the wavelength slope of the emissivity. All of the above analysis was repeated for an emissivity increasing with wavelength. There was a slight reduction in the standard deviations at high temperatures, but otherwise all results were qualitatively the same.

Logarithmic amplifiers are quite undesirable because of the penalty in precision.

Comparison of Figs. 3 and 14 shows that whether the errors are of the relative or absolute type, the greatest emissivity shift from the true values occurs for the shortest wavelengths and the highest temperatures.

Gardner [3] also studied least-squares fitted multiwavelength pyrometry using six wavelengths and unweighted fits, linear amplifiers, and uniformly distributed random relative errors. He assumed the logarithm of the emissivity to be a linear function of wavelength and used the Wien approximation. The temperature range 600 to 1600 K was considered, and two emissivity models were used: a gray body with $\varepsilon = 0.5$ and tungsten. He also examined the influence of spectral span, using both the range 750 to 1000 nm and the range 750 to 1600 nm. The errors increased three- to fourfold for the shorter interval. His study used only 10 runs to calculate the mean and standard deviation for the temperature, however. This is not statistically significant for examining improvement achieved by increasing the number of wavelengths used, since one must study a second-order effect: variation in the variance.

Gardner et al. [4] built an instrument utilizing the design considered and used it to measure surface temperatures for various metals.

Coates [5] also studied the least-squares approach to multiwavelength pyrometry using the Wien approximation, and taking the logarithm of the emissivity as a linear function of wavelength. He concluded that a narrow-band pyrometer, with a crude estimate of the emissivity, will in general yield a more reliable estimate of the temperature than any form of multi-wavelength pyrometer. These conclusions are consistent with this work. Beyond about four wavelengths, little further improvement is seen. In situations where the emissivity is unknown, and expected to be a function of wavelength, multiwavelength pyrometry assuming a linear variation with wavelength for the logarithm of the emissivity can be expected to give better results than the graybody assumption, provided the emissivity model is reasonable for the portion of the spectrum considered.

ACKNOWLEDGMENT

This work was performed under the auspices of the U.S. Department of Energy by the Lawrence Livermore National Laboratory under Contract W-7405-ENG-48.

REFERENCES

1. J. Hiernaut, R. Beuker, W. Heinz, R. Selfslag, and M. Hoch, *High Temp.-High Press.* **18**:617 (1986).
2. J. Hiernaut, F. Sakuma, and C. Ronchi, *High Temp.-High Press.* **21**:139 (1989).
3. J. L. Gardner, *High Temp.-High Press.* **12**:699 (1980).
4. J. L. Gardner, T. P. Jones, and M. R. Davies, *High Temp.-High Press.* **13**:459 (1981).
5. P. B. Coates, *High Temp.-High Press.* **20**:433 (1988).

Printed in Belgium